ARC Centre of Excellence in Population Ageing Research

Working Paper 2018/3

Market Price of Longevity Risk for A Multi-Cohort Mortality Model with Application to Longevity Bond Option Pricing

Yajing Xu[1], Michael Sherris[2] and Jonathan Ziveyi[3]

[1]Ernst and Young, Shanghai, Email: yajing.xu@hotmail.com

[2]School of Risk and Actuarial Studies, Centre of Excellence in Population Ageing Research (CEPAR), UNSW Australia, Sydney, Australia. Email: m.sherris@unsw.edu.au

[3]School of Risk and Actuarial Studies, Centre of Excellence in Population Ageing Research (CEPAR), UNSW Australia, Sydney, Australia. Email: j.ziveyi@unsw.edu.au

Market Price of Longevity Risk for A Multi-Cohort Mortality Model with Application to Longevity Bond Option Pricing

Yajing Xu[*], Michael Sherris [†]and Jonathan Ziveyi [‡]

February 2018

Abstract

The pricing of longevity-linked securities depends not only on the stochastic uncertainty of the underlying risk factors, but also the attitude of investors towards those factors. In this research, we investigate how to estimate the market risk premium of longevity risk using investable retirement indexes, incorporating uncertain real interest rates using an affine dynamic Nelson-Siegel model. A multi-cohort aggregate, or systematic, continuous time affine mortality model is used where each risk factor is assigned a market price of mortality risk. To calibrate the market price of longevity risk, a common practice is to make use of market prices, such as longevity-linked securities and longevity indices. We use the BlackRock CoRI Retirement Indexes, which provides a daily level of estimated cost of lifetime retirement income for 20 cohorts in the U.S. Although investment in the index directly is not possible, individuals can invest in funds that track the index. For these 20 cohorts, we assume risk premiums for the common factors are the same across cohorts, but the risk premium of the factors for a specific cohort is allowed to take different values for different cohorts. The market prices of longevity risk are then calibrated by matching the risk-neutral model prices with BlackRock CoRI index values. Closed-form expressions and prices for European options on longevity zero-coupon bonds are derived using the model and compared to prices for standard options on zero coupon bonds. The impact of uncertain mortality on long term option prices is quantified and discussed.

Keywords: Multi-cohort mortality model; Market price of longevity risk; Longevity indexes.

[*]EY Shanghai, email: yajing.xu@hotmail.com, phone: (61)0431060127.

[†]Corresponding author: School of Risk & Actuarial Studies, Australian Research Council Centre of Excellence in Population Ageing Research (CEPAR), UNSW Sydney, email: m.sherris@unsw.edu.au, phone: (61)0449890480.

[‡]School of Risk & Actuarial Studies, Australian Research Council Centre of Excellence in Population Ageing Research (CEPAR), UNSW Sydney, email:j.ziveyi@unsw.edu.au, phone: (61) 2 9385 8006.

1 Introduction

Life insurance companies and defined benefit (DB) pension plans are exposed to systematic longevity risk which is the unanticipated changes in mortality rates that cannot be averaged out by applying the law of large numbers. This risk should be reflected in market pricing of longevity–linked products. Changes in accounting and solvency regulatory requirements have shifted the focus to the market valuation of these liabilities, yet there remains no actively traded market to price the systematic risk.

The development of longevity-linked securities and derivatives aims to allow the management of this risk as well as provide market based prices. For example, Blake and Burrows (2001) propose the transfer of this risk to the financial market using longevity bonds. Other proposed instruments include survivor swaps (Dowd et al., 2006), q-forwards (Coughlan et al., 2007) and mortality linked options (Bauer et al., 2010). Financial markets have the capacity and experience in risk management to take on longevity risk which in the past has mostly been reinsured.

The pricing of longevity-linked securities depends not only on the stochastic process for the underlying risk factors, but also the attitude of investor towards the risk of those factors. The Life & Longevity Markets Association (LLMA) has identified the market risk premium of longevity risk as one of the key inputs in a longevity pricing framework[1]. To determine the market risk premium, a common practice is to use available market prices, such as life annuities, longevity-linked securities and longevity indices. The longevity market is however incomplete due to the lack of traded assets, and calibration of market prices of risk is problematic.

In an incomplete market, longevity-linked derivatives pricing usually involves making assumptions about the market risk premium of bearing longevity risk directly or implicitly. Lin and Cox (2005) propose to use a Wang transform for the securitization of longevity risk,

[1] LLMA(2010). Longevity Pricing Framework. [www.llma.org]

and the market price is defined as the shift parameter in the Wang transform to risk adjust a survival distribution based on 1996 IAM 2000 Basic Table and annuity quotes. A different approach is taken in Bauer and Ruß (2006) and Chigodaev et al. (2016), who propose to derive parameter values for stochastic mortality models using survival probabilities implied by annuity prices, so that the market price of longevity risk is implicitly included in these parameter values. The Wang transform has limitations in pricing longevity risk (Bauer et al., 2010). There remains no well accepted method to calibrate and incorporate the market price of longevity risk into mortality dynamics under a risk-neutral measure for market valuation that can be used in modelling and pricing of longevity-linked products.

The present paper aims to fill this gap using a pricing framework for stochastic mortality based on affine processes which have been used extensively in modelling interest rate dynamics (Duffie et al., 1996; Dai and Singleton, 2000; Duffee, 2002), as well as for stochastic mortality (Blackburn and Sherris, 2013; Jevtic et al., 2013; Xu et al., 2015). The benefits of these processes are in the analytical tractability and ease of application to valuation and risk management of longevity linked product and financial instruments.

We are the first to derive the market risk premium of longevity risk using investable retirement indices. The BlackRock CoRI Retirement Indexes provide a daily level of the estimated cost of lifetime retirement income for 20 cohorts in the U.S. The CoRI Indexes are designed to help investors estimate the cost of providing retirement income and assist in planning for future income goals. Key factors taken into account in the indices include current interest rates, inflation expectations and life expectancy. Investors can use the CoRI Indices as a risk metric directly or can invest in the BlackRock CoRI Funds that track the indices.

Since the CoRI Indexes consist of 20 cohorts, we use the multi-cohort mortality model developed by Xu et al. (2015), in which the dynamics of each cohort are driven by two common factors and a cohort specific factor. In the financial literature, the market price of risk is normally obtained by specifying the dynamics of state variables under both an objective probability measure and an equivalent martingale measure. The affine mortality model allows us to calibrate the market price of longevity risk in a similar way. To change between the best-estimate measure and the risk-neutral measure, we assign each factor a market price of risk. Since the instantaneous volatility of each factor is assumed to be constant, the subtraction of the product of market price of risk and volatility from the drift under the best-estimate measure results in a process that is also affine.

Option-type longevity derivatives are considered in Bauer et al. (2010), where the underlying asset is the survival probability at maturity. Bauer et al. (2010) note that options are desirable hedging instruments and significantly reduce the committed capital compared to longevity bonds. With calibrated market price of longevity risk, we derive closed-form expressions for prices of options on longevity zero-coupon bonds and discuss the impact of stochastic mortality on these option prices. We show that call prices on longevity bonds are increasing functions of the option maturity. However, with an increase in bond maturity, call prices increase first and decrease thereafter. We compare the prices of longevity zero-coupon bond options with the prices of zero-coupon bond options. For shorter bond maturities zero-coupon bond options are lower while for longer maturities longevity linked zero-coupon bond options are lower.

The paper will introduce the modelling framework and the structure of the longevity indexes, which is a sum of longevity bonds with different maturities. We will present the estimation results for mortality and interest rate models, and calibrate the market prices of longevity risk using the CoRI Retirement Indexes. We present derivations in closed-form for prices of longevity bond options expressions and discuss the impact of stochastic mortality on these options.

2 Blackrock CORI Retirement Indexes

We use the BlackRock CoRI Retirement Indexes to imply a market price of longevity risk, which can then be used to assess the risk premiums for mortality risk when pricing derivative securities written on longevity-linked instruments. BlackRock, which is one of the leading global asset manager, has tried for many years to introduce new and innovative approaches to address the challenge of converting retirement savings account balances into lifetime income streams. In June 2013, BlackRock introduced the CoRI Indexes to help investors estimate and track the cost of $1 of annual lifetime income at retirement. The CoRI consists of twenty indexes corresponding to twenty cohorts born from 1941 to 1960 in U.S. For cohorts with an age below 65 the index is the discounted cost of purchasing inflation-adjusted lifetime retirement income at age 65, and for other cohorts it is the cost of purchasing inflation-adjusted retirement income for remaining life.

The CoRI indexes aim to help investors improve the way they plan for retirement. Investors can use the CoRI index as a risk metric directly or invest in the BlackRock CoRI Funds that track the index. To help investors prepare for retirement, BlackRock also launched five CoRI funds. The CoRI funds are comprised of CoRI 2015, 2017, 2019, 2021, and 2023 funds that track the corresponding CoRI indexes. The CoRI indexes are constructed based on real-time market data, and they do not include any fees or premium taxes that would be associated with the price of an annuity. Although the indexes are not tradeable, they can be invested in and provide a more suitable basis for implying market prices of risk than life annuity quotes.

BlackRock do not provide the details of the cash flow modelling and actuarial techniques used to construct the indexes. The funds that track the Indexes are constructed using liability-driven investment techniques. They consist of investment grade corporate bonds, U.S. government bonds and U.S. Treasury STRIPS and take into account the factors that life annuity providers use including life expectancy, interest rates and inflation expectations.

We use market based models for stochastic mortality taking into account longevity expectations as well as models of the term structure of real interest rates accounting for inflation expectations. The models are calibrated to historical U.S. cohort mortality data and market based U.S. real interest rates. These are used to construct indexes that reflect the same factors as the BlackRock indexes.

3 Longevity Index Construction

The Indexes are constructed on complete filtered probability space $(\Omega, \mathcal{F}, \mathbf{F}, P)$, where Ω is the set of possible states of nature, $\mathbf{F} = \{\mathcal{F}_t\}_{0 \leq t \leq T}$, and P is interpreted as the objective probability measure. We assume that $\mathbf{F}$ is the natural filtration generated by two independent multi-dimensional standard Wiener processes W_r and W_μ. Set $\mathcal{F}_t = \mathcal{G}_t \vee \mathcal{H}_t$ where $\mathcal{G}_t$ and $\mathcal{H}_t$ contain the information concerning the financial and mortality markets, respectively. Thus $\mathbf{G}$ and $\mathbf{H}$ are independent and generated by W_r and W_μ respectively.

The longevity index requires a market model for mortality and real interest rates. These are used to determine the value of zero coupon longevity bonds that have a payment based on the realised proportion of survivors of a particular cohort at a specified future time. The value of the stream of the lifetime income stream that forms the index is just a sum of these zero coupon longevity bonds. We first specify the models.

3.1 Mortality Model

We use the multi-cohort mortality model developed by Xu et al. (2015). The model is a three-factor affine mortality model in which the mortality intensity process for each cohort i aged $x + t$ at time t is modelled via

$$\mu^i(x,t) = X_1(t) + X_2(t) + Z^i(t), \tag{1}$$

where $X_1(t)$, $X_2(t)$ are two common factors and $Z^i(t)$ is the cohort specific factor. The model is parsimonious and provides closed form solutions for survival probabilities allowing efficient calibration and computation of zero coupon longevity bond prices.

Under the best-estimate measure, which reflects future expected mortality based on historical trends, $\bar{Q}$, the state variables $(X_1(t), X_2(t), Z^i(t))$ have the following dynamics

$$dX_j(t) = -\phi_j X_j(t)dt + \sigma_j dW_j^{\bar{Q}}(t), j = 1, 2, \tag{2}$$

$$dZ^i(t) = -\phi_3^i Z^i(t)dt + \sigma_3^i dW_3^{\bar{Q},i}(t), \tag{3}$$

where ϕ_1, ϕ_2, ϕ_3^i, σ_1, σ_2 and σ_3^i are constants, and $W_1^{\bar{Q}}(t)$, $W_2^{\bar{Q}}(t)$ and $W_3^{\bar{Q},i}(t)$ are standard Wiener processes under $\bar{Q}$.

Denote the best-estimate survival probability by $S^{\bar{Q},i}(x, t, T)$ for cohort i aged x at time t over duration $T - t$. From Xu et al. (2015), this probability has a closed-form solution such that

$$\begin{aligned} S^{\bar{Q},i}(x, t, T) &= E^{\bar{Q}}[e^{-\int_t^T \mu^i(x,s)ds} | \mathcal{F}_t] \\ &= e^{B_1(t,T)X_1(t) + B_2(t,T)X_2(t) + B_3^i(t,T)Z^i(t) + A^i(t,T)}, \end{aligned} \tag{4}$$

where

$$\begin{aligned} B_1(t, T) &= -\frac{1 - e^{-\phi_1(T-t)}}{\phi_1}, \quad B_2(t, T) = -\frac{1 - e^{-\phi_2(T-t)}}{\phi_2}, \quad B_3^i(t, T) = -\frac{1 - e^{-\phi_3^i(T-t)}}{\phi_3^i}, \\ A^i(t, T) &= \frac{1}{2}\sum_{j=1}^{2} \frac{\sigma_j^2}{\phi_j^3} \left[\frac{1}{2}(1 - e^{-2\phi_j(T-t)}) - 2(1 - e^{-\phi_j(T-t)}) + \phi_j(T - t)\right] \\ &\quad + \frac{1}{2}\frac{(\sigma_3^i)^2}{(\phi_3^i)^3} \left[\frac{1}{2}(1 - e^{-2\phi_3^i(T-t)}) - 2(1 - e^{-\phi_3^i(T-t)}) + \phi_3^i(T - t)\right]. \end{aligned} \tag{5}$$

As discussed in Xu et al. (2015), so far the dynamics are specified under the best-estimate measure $\bar{Q}$ and the parameters are estimated using observed mortality data. In order to account for a risk premium, we use the Girsanov's theorem to change to the pricing risk-neutral measure Q. We assume $\Lambda^i = (\lambda_{\mu,1}, \lambda_{\mu,2}, \lambda^i_{\mu,3})^T$ to be the vector of market price of risk associated with cohort i (see the completely affine market price of risk specification in Dai and Singleton (2000) and Duffee (2002)). The market prices of longevity risk, $\lambda_{\mu,1}$ and $\lambda_{\mu,2}$ are assumed to be the same across cohorts as they are associated with the common factors, but $\lambda^i_{\mu,3}$ is allowed to take different values for different cohorts. By using the Girsanov's Theorem we have

$$dW_j^Q(t) = dW_j^{\bar{Q}}(t) + \lambda_{\mu,j}dt, j = 1, 2 \tag{6}$$

$$dW_3^{Q,i}(t) = dW_3^{\bar{Q},i}(t) + \lambda^i_{\mu,3}dt \tag{7}$$

where $W_1^Q(t)$, $W_2^Q(t)$ and $W_3^{Q,i}(t)$ are standard Wiener processes under the risk-neutral measure Q. Thus the dynamics of mortality intensity under the risk-neutral measure Q are given by

$$\begin{aligned} d\mu^i(x,t) = & \left[-\phi_1 X_1(t) - \phi_2 X_2(t) - \phi_3^i Z^i(t) - \sigma_1\lambda_{\mu,1} - \sigma_2\lambda_{\mu,2} - \sigma_3^i\lambda^i_{\mu,3}\right] dt \\ & + \sigma_1 dW_1^Q(t) + \sigma_2 dW_2^Q(t) + \sigma_3^i dW_3^{Q,i}(t). \end{aligned} \tag{8}$$

The risk-neutral survival probability is

$$\begin{aligned} S^{Q,i}(x,t,T) &= E^Q\left[\mathrm{e}^{-\int_t^T \mu^i(x,s)ds}|\mathcal{H}(t)\right] \\ &= \mathrm{e}^{B_1(t,T)X_1(t)+B_2(t,T)X_2(t)+B_3^i(t,T)Z^i(t)+A^i(t,T)+C^i(t,T)} \\ &= S^{\bar{Q},i}(x,t,T)\mathrm{e}^{C^i(t,T)}, \end{aligned} \tag{9}$$

where

$$C^i(t,T) = \sum_{j=1}^{2} \frac{\sigma_j\lambda_{\mu,j}}{\phi_j^2}\left[\phi_j(T-t) - \left(1 - \mathrm{e}^{-\phi_j(T-t)}\right)\right] + \frac{\sigma_3^i\lambda^i_{\mu,3}}{(\phi_3^i)^2}\left[\phi_3^i(T-t) - \left(1 - \mathrm{e}^{-\phi_3^i(T-t)}\right)\right].$$

3.2 Interest Rate Model

For interest rates, we choose the arbitrage-free Nelson-Siegel (AFNS) model developed by Christensen et al. (2011) due to its good empirical fit and arbitrage-free property. Diebold and Li (2006) introduce dynamics to the yield curve model of Nelson and Siegel (1987) and show that this model provides a good empirical fit. Based on Diebold and Li (2006), Christensen et al. (2011) prove that with a time-invariant yield-adjustment term the empirical successful dynamic Nelson-Siegel (DNS) model can be made arbitrage-free. The AFNS model combines the DNS factor loading structure and the arbitrage-free property of an affine term structure model. We use the independent-factor AFNS model since it outperforms the correlated-factor AFNS model in out-of-sample forecasts (Christensen et al., 2011).

Let $P(t,T)$ denote the price of a discount bond with maturity of $T-t$, and $y(t,T)$ be its continuously compounded yield to maturity, then by definition we have

$$P(t,T) = \mathrm{e}^{-(T-t)y(t,T)}. \tag{10}$$

Christensen et al. (2011) propose the following representation for the yield function,

$$y(t,T) = L(t) + \frac{1-e^{-\lambda(T-t)}}{\lambda(T-t)}S(t) + \left[\frac{1-e^{-\lambda(T-t)}}{\lambda(T-t)} - e^{-\lambda(T-t)}\right]C(t) - \frac{V(t,T)}{T-t}, \tag{11}$$

where λ is the Nelson-Siegel parameter, and $-\frac{V(t,T)}{T-t}$ is the yield-adjustment term. In the independent-factor case the yield-adjustment term is

$$
\begin{aligned}
-\frac{V(t,T)}{T-t} = &-\frac{(T-t)^2}{6}(s_1)^2 \\
&-\left[\frac{1}{2(\lambda)^2} - \frac{1}{(\lambda)^3}\frac{1-e^{-\lambda(T-t)}}{(T-t)} + \frac{1}{4(\lambda)^3}\frac{1-e^{-2\lambda(T-t)}}{(T-t)}\right](s_2)^2 \\
&-\left[\frac{1}{2(\lambda)^2} + \frac{1}{(\lambda)^2}e^{-\lambda(T-t)} - \frac{1}{4\lambda}(T-t)e^{-2\lambda(T-t)} - \frac{3}{4(\lambda)^2}e^{-\lambda(T-t)}\right. \\
&\left.\quad -\frac{2}{(\lambda)^3}\frac{1-e^{-\lambda(T-t)}}{(T-t)} + \frac{5}{8(\lambda)^3}\frac{1-e^{-2\lambda(T-t)}}{(T-t)}\right](s_3)^2,
\end{aligned}
$$

where s_1, s_2 and s_3 are volatility parameters.

In the above equation, $L(t)$, $S(t)$ and $C(t)$ are the time-varying level, slope and curvature factors with the following dynamics under the risk-neutral Q-measure

$$
\begin{pmatrix} dL(t) \\ dS(t) \\ dC(t) \end{pmatrix} = -\begin{pmatrix} 0 & 0 & 0 \\ 0 & \lambda & -\lambda \\ 0 & 0 & \lambda \end{pmatrix}\begin{pmatrix} L(t) \\ S(t) \\ C(t) \end{pmatrix} dt + \begin{pmatrix} s_1 & 0 & 0 \\ 0 & s_2 & 0 \\ 0 & 0 & s_3 \end{pmatrix}\begin{pmatrix} d\tilde{W}_1^Q(t) \\ d\tilde{W}_2^Q(t) \\ d\tilde{W}_3^Q(t) \end{pmatrix}, \tag{12}
$$

while under the real-world probability measure these factors evolve as follows

$$
\begin{pmatrix} dL(t) \\ dS(t) \\ dC(t) \end{pmatrix} = \begin{pmatrix} \kappa_1 & 0 & 0 \\ 0 & \kappa_2 & 0 \\ 0 & 0 & \kappa_3 \end{pmatrix}\left[\begin{pmatrix} \theta_1 \\ \theta_2 \\ \theta_3 \end{pmatrix} - \begin{pmatrix} L(t) \\ S(t) \\ C(t) \end{pmatrix}\right] dt + \begin{pmatrix} s_1 & 0 & 0 \\ 0 & s_2 & 0 \\ 0 & 0 & s_3 \end{pmatrix}\begin{pmatrix} d\tilde{W}_1^P(t) \\ d\tilde{W}_2^P(t) \\ d\tilde{W}_3^P(t) \end{pmatrix}, \tag{13}
$$

where κ_1, κ_2, κ_3, θ_1, θ_2 and θ_3 are real-world parameters.

3.3 The Longevity Index

We define a longevity zero-coupon bond $\bar{P}_x^i(t,T)$, which pays the realized proportion of the initial population in cohort i that is alive at time T, as our basic instrument. The definition of $\bar{P}_x^i(t,T)$ is similar to the definition of a defaultable zero-coupon bond (as defined in

Schönbucher (2003)), where the mortality intensity corresponds to the default intensity. The price of a longevity zero-coupon bond can be explicitly represented as

$$\begin{aligned}\bar{P}_x^i(t,T) &= E^Q\left[\mathrm{e}^{-\int_t^T\left(r(s)+\mu^i(x,s)\right)ds}|\mathcal{F}(t)\right]\\ &= E^Q\left[\mathrm{e}^{-\int_t^T r(s)ds}|\mathcal{G}(t)\right]E^Q\left[\mathrm{e}^{-\int_t^T \mu^i(x,s)ds}|\mathcal{H}(t)\right]\\ &= P(t,T)S^{Q,i}(x,t,T), \end{aligned} \tag{14}$$

since we assume that the dynamics of the mortality rates and the dynamics of the interest rates are independent.

Taking the longevity zero-coupon bond as a starting point, a longevity index that pays the discounted value of lifetime annual income of \$1 for cohort i is just a portfolio of longevity bonds of different maturities. Thus the value of the longevity index can be represented as a sum of longevity bond prices

$$I_x^i(t) = \sum_{j=1}^{x^*-x} \bar{P}_x^i(t,t+j), \tag{15}$$

where x^* is the maximum age.

4 Model Estimation and Market Price of Risk for Longevity

We provide the estimation results for the multi-cohort mortality model and the AFNS interest rate model which we use to contruct the Longevity Indexes. We derive the implied market prices of longevity risk from the CoRI Retirement Indexes.

4.1 Estimation of the Mortality Model

We use the U.S. male mortality data from Human Mortality Database from 1934 to 2013, aged 50 to 100. The mortality data is restructured on a cohort basis. The observed survival probability for cohort i aged x at time t over duration $T-t$ is calculated by

$$\tilde{S}^i(x,t,T) = \prod_{s=1}^{T-t}(1-\tilde{q}_x^i(t+s-1)), \tag{16}$$

where $\tilde{q}_x^i(t)$ is the observed death rate at time t. The corresponding observed average force of mortality is defined as

$$\tilde{\mu}^i(x,t,T) = -\frac{1}{T-t}\log\tilde{S}^i(x,t,T). \tag{17}$$

Figure 1 shows the average force of mortality in U.S. for cohorts born between 1884 and 1913, aged 50 to 100.

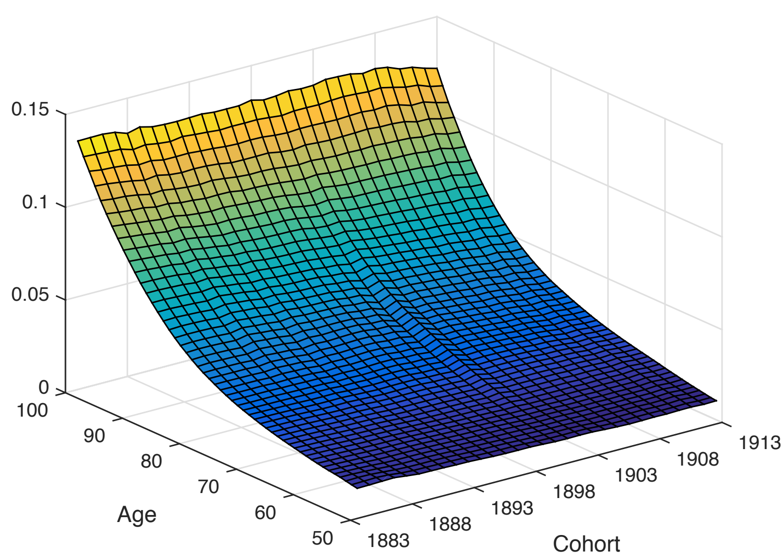

Figure 1: Male average force of mortality in U.S. for cohorts born between 1884 and 1913, aged 50 to 100.

The parameters for two common factors are estimated using a Kalman filter method (maximum likelihood). The measurement equation can be represented as

$$y_t = -BX_t - A + \varepsilon_t, \qquad \varepsilon_t \sim N(0, H), \tag{18}$$

where

$$B = -\begin{pmatrix} \frac{1-e^{-\phi_1}}{\phi_1} & \frac{1-e^{-\phi_2}}{\phi_2} \\ \frac{1-e^{-2\phi_1}}{2\phi_1} & \frac{1-e^{-2\phi_2}}{2\phi_2} \\ \vdots & \vdots \\ \frac{1-e^{-n\phi_1}}{n\phi_1} & \frac{1-e^{-n\phi_2}}{n\phi_2} \end{pmatrix}, \quad A = \begin{pmatrix} \frac{1}{2}\sum_{i=1}^{2} \frac{\sigma_i^2}{\phi_i^3}[\frac{1}{2}(1-e^{-2\phi_i}) - 2(1-e^{-\phi_i}) + \phi_i] \\ \frac{1}{2}\sum_{i=1}^{2} \frac{\sigma_i^2}{2\phi_i^3}[\frac{1}{2}(1-e^{-4\phi_i}) - 2(1-e^{-2\phi_i}) + 2\phi_i] \\ \vdots \\ \frac{1}{2}\sum_{i=1}^{2} \frac{\sigma_i^2}{n\phi_i^3}[\frac{1}{2}(1-e^{-2n\phi_i}) - 2(1-e^{-n\phi_i}) + n\phi_i] \end{pmatrix},$$

and where H is the covariance matrix for the Gaussian observation noise. Since the volatility of the measurement error varies with age, we assume H to be an n-dimensional diagonal matrix with elements $\sigma_\varepsilon^2(i)$ $(i = 1, 2, ..., n)$ taking an exponential form,

$$\sigma_\varepsilon^2(i) = \varepsilon_1 \exp(\varepsilon_2 i), \tag{19}$$

where ε_1 and ε_2 are two constants. With this specification the volatility of the measurement error is exponentially increasing with age.

The state variables evolve on the time dimension, and the transition equation can be represented as

$$X_t = \Phi X_{t-1} + \eta_t, \qquad \eta_t \sim N(0, Q), \tag{20}$$

where $\Phi = \begin{pmatrix} e^{-\phi_1} & 0 \\ 0 & e^{-\phi_2} \end{pmatrix}$, $Q = \begin{pmatrix} \frac{\sigma_1^2}{2\phi_1}(1-e^{-2\phi_1}) & 0 \\ 0 & \frac{\sigma_2^2}{2\phi_2}(1-e^{-2\phi_2}) \end{pmatrix}$.

Using the Kalman filter method, we obtain the estimation results of the two common factors as shown in Table 1. The model captures the improvement trend with mean reverting factors as well as the exponentially increasing "Poisson" variation in the measurement equation.

The parameters associated with cohort factors are estimated by minimising the calibration

Table 1: Kalman filter parameter estimates, log likelihood and RMSE.

ϕ_1	-0.14313
ϕ_2	-0.07904
σ_1	0.00006
σ_2	0.00018
$\varepsilon_1(\times 10^7)$	2.74881
$\varepsilon_2(\times 10^7)$	1.99699
Log likelihood	24440
RMSE	0.00051

error given the common factors. We assume the values of these parameters remain the same across 10 cohorts to reduce the number of parameters and improve estimation efficiency. Cohorts close together exhibit similar mortality improvements. We show estimation results for cohorts with a 10-year interval in Table 2. Trend and volatility parameters have reduced for later cohorts. The most recent 1904–1913 group of 10 cohorts have the lowest estimated volatility reflecting changes in cohort mortality. We use these most recent parameters in our market price of risk estimation.

Table 2: Estimation results for cohort specific factors with a 10-year interval.

i cohort	ϕ_3^i	σ_3^i	Z^i
1884-1893	0.06791	0.00558	0.00163
1894-1903	0.05228	0.00719	0.00106
1904-1913	0.05463	0.00122	-0.00079

Figure 2 plots the mean absolute percentage error (MAPE) per age of the estimated survival probabilities for all the cohorts. The MAPEs are low even at very high ages, which indicates a good empirical fit of the model. One factor that accounts for these older age variations is mortality heterogeneity that is not captured in models of systematic mortality.

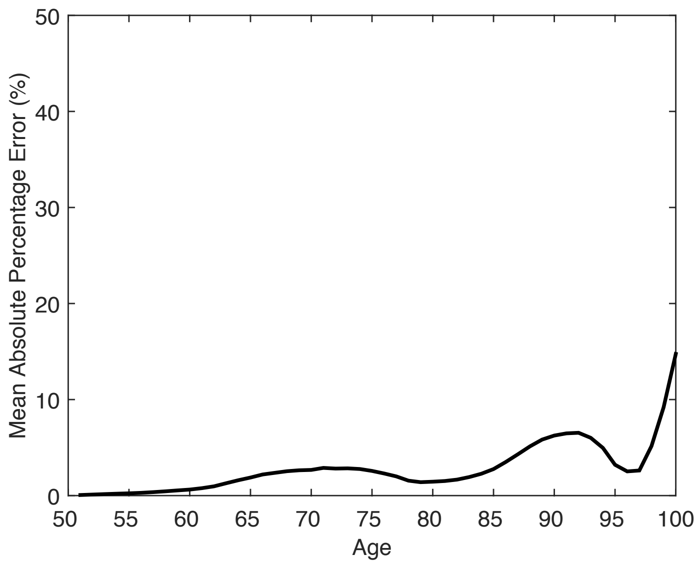

Figure 2: Mean percentage error of estimated survival probabilities.

4.2 Estimation of the Interest Rate Model

As mortality-linked claims are long dated and the lifetime income stream is indexed to inflation, we take into account changes in inflation in the modelling framework. We model real interest rates and use end-of-month observations for real yields on Treasury Inflation Protected Securities (TIPS) interpolated by the U.S. Treasury. TIPS are indexed to inflation as defined by the Consumer Price Index (CPI) so that they eliminate the inflation risk and provide a real rate of return. Until the end of January 2010, the U.S. Treasury issued TIPS at fixed maturities, 5, 7, 10 and 20 years. On February 22, 2010, they sold a new TIP security with a maturity time of 30 years. We use the Treasury real yield curve rates at 5 maturities of 5, 7, 10 20, and 30 years from February 2010 to March 2015.

Figure 3 shows the monthly yield curve rates and Table 3 presents corresponding descriptive statistics. We see that during this period real interest rates were negative and there has been auto–regressive behaviour across the term structure.

The AFNS model is represented in a state-space form and estimated using a Kalman filter

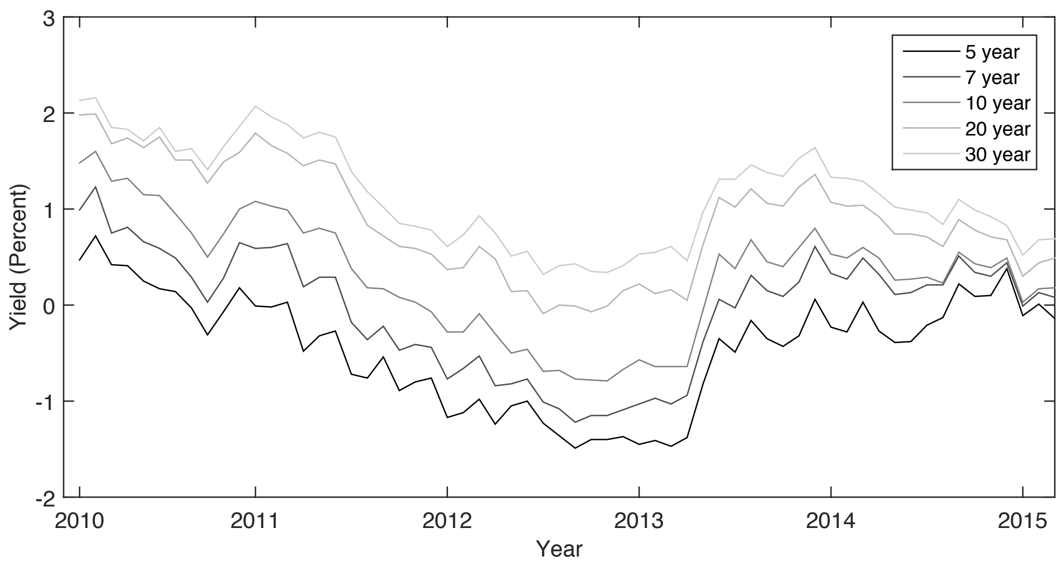

Figure 3: Time series of U.S. real yield curve rates, from February 2010 to March 2015.

Table 3: Descriptive statistics of U.S. real yield curve rates, $\hat{\rho}(i)$ denotes the sample autocorrelation with a time-lag of i months.

Maturity	Mean	Std. Dev.	Min.	Max.	$\hat{\rho}(1)$	$\hat{\rho}(6)$	$\hat{\rho}(12)$
5Y	-0.4497	0.5955	-1.49	0.72	0.9037	0.5825	0.1160
7Y	-0.0461	0.6281	-1.22	1.23	0.9163	0.5814	0.0607
10Y	0.2984	0.6245	-0.79	1.60	0.9204	0.5568	0.0619
20Y	0.8790	0.5834	-0.09	1.99	0.9180	0.5715	0.0356
30Y	1.1452	0.5284	0.32	2.16	0.9137	0.5183	0.0094

algorithm. The measurement equation is

$$y_t = -BY_t - A + \varepsilon_t, \qquad \varepsilon_t \sim N(0, H), \tag{21}$$

where

$$y_t = \begin{pmatrix} y_t(\tau_1) \\ \vdots \\ y_t(\tau_k) \end{pmatrix}, \quad B = -\begin{pmatrix} 1 & \frac{1-e^{-\lambda\tau_1}}{\lambda\tau_1} & \frac{1-e^{-\lambda\tau_1}}{\lambda\tau_1} - e^{-\lambda\tau_1} \\ \vdots & \vdots & \vdots \\ 1 & \frac{1-e^{-\lambda\tau_k}}{\lambda\tau_k} & \frac{1-e^{-\lambda\tau_k}}{\lambda\tau_k} - e^{-\lambda\tau_k} \end{pmatrix}, \quad Y_t = \begin{pmatrix} L(t) \\ S(t) \\ C(t) \end{pmatrix}, \quad A = \begin{pmatrix} \frac{V(\tau_1)}{\tau_1} \\ \vdots \\ \frac{V(\tau_k}{\tau_k} \end{pmatrix}.$$

The state transition equation is

$$Y_t = (I - \mathrm{e}^{-K\Delta t})\Theta + \mathrm{e}^{-K\Delta t} Y_{t-1} + \eta_t, \qquad \eta_t \sim N(0, Q), \tag{22}$$

where

$$K = \begin{pmatrix} \kappa_1 & 0 & 0 \\ 0 & \kappa_2 & 0 \\ 0 & 0 & \kappa_3 \end{pmatrix}, \quad \Theta = \begin{pmatrix} \theta_1 \\ \theta_2 \\ \theta_3 \end{pmatrix},$$

and $Q = \int_0^{\Delta t} \mathrm{e}^{-Ks} \Sigma \Sigma^{\mathrm{T}} \mathrm{e}^{-(K^{\mathrm{T}} s)} ds$ with

$$\Sigma = \begin{pmatrix} s_1 & 0 & 0 \\ 0 & s_2 & 0 \\ 0 & 0 & s_3 \end{pmatrix}.$$

Since we use monthly data, $\Delta t = \frac{1}{12}$.

Estimates for the independent-factor AFNS model are given in Table 4. For the in-sample fit, residual means and their root mean square errors (RMSEs) are provided in Table 5. The RMSEs are consistent with the results obtained in Christensen et al. (2011), which are typically less than ten basis points. There is no apparent maturity-dependent trend in

RMSEs, which indicates that the model fits yields with long maturities as well as shorter maturities. Using the estimates from Table 4, Figure 4 plots the mean fitted curve for the independent-factor AFNS model. The figure shows small differences between the AFNS mean yield curve and the observed mean yield curve, which also indicates model goodness-of-fit.

For the AFNS model, after having calibrated the model, the evolution of future yield curve can be forecast using Equation (11). Figure 5 shows the forecast yield curve at the end of March 2015.

Table 4: Estimated independent-factor AFNS model. The estimated λ is 0.7204, and the maximized log likelihood is 1622.75.

i	κ_i	θ_i	s_i
1	0.0458	0.0723	0.0061
2	0.1958	-0.0231	0.0047
3	1.2237	-0.0134	0.0059

Table 5: Residual means and their root mean square errors for maturities measured in years. Means and RMSE's are in basis points.

Maturity	Mean	RMSE
5Y	-2.16	6.76
7Y	1.28	7.87
10Y	2.46	6.11
20Y	6.97	5.58
30Y	-8.69	6.36

4.3 Market Price of Longevity Risk

The BlackRock CoRI index levels are based on real-time market data and are calculated using a variety of factors including starting level, inflation, risk, interest rates and life expectancy. The CoRI index level reflects current market information about what insurers are charging to manage similar risks. We take into account all of these factors. In order to imply market

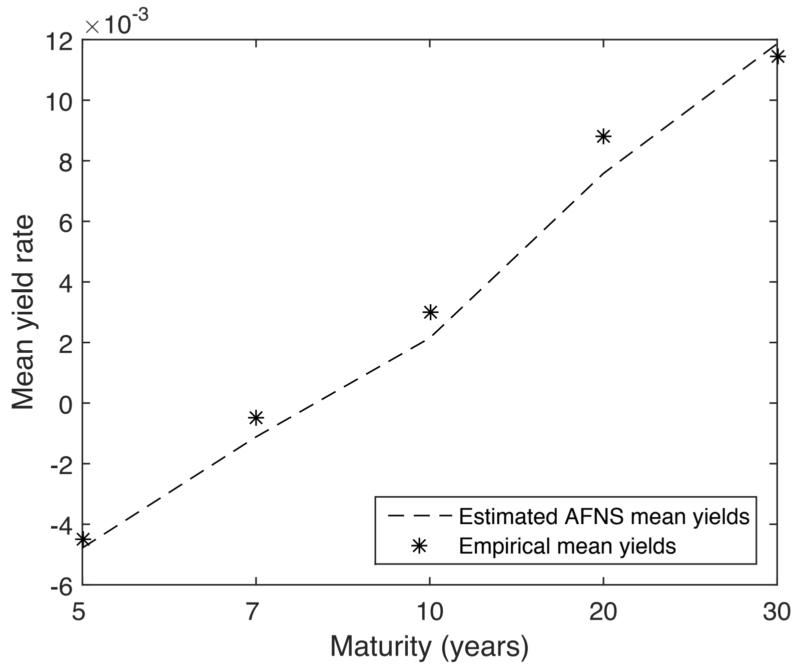

Figure 4: Empirical mean yield curve and the fitted AFNS mean yield curve, average from February 2010 to March 2015. Mean yields are in decimals.

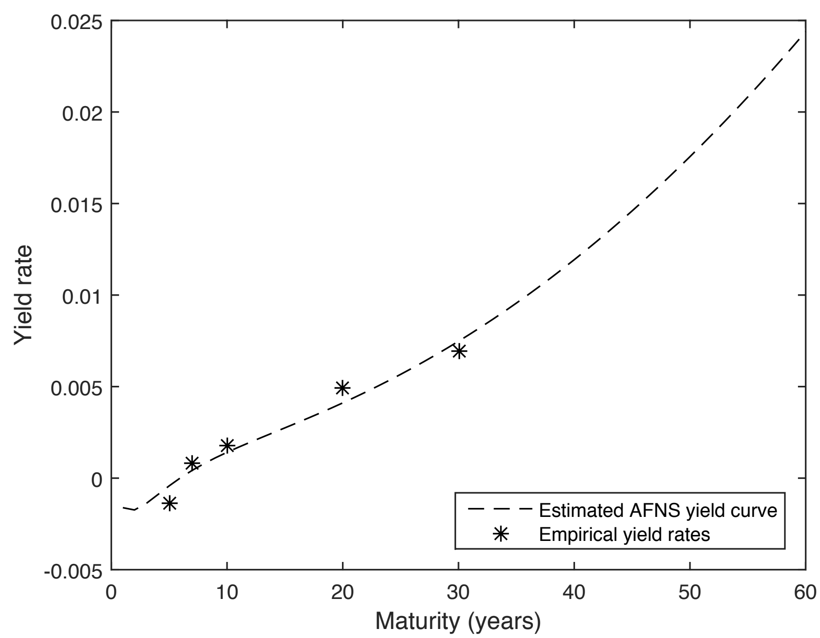

Figure 5: Empirical yield rates and the fitted AFNS yield curve at the end of March 2015. Yields are in decimals.

prices of longevity risk from the CORI indexes, we minimize differences between our longevity index values and the CoRI index values as given in Equations (23) and (24).

The CoRI indexes do not differentiate index values for males and females. We use male mortality data since it is common practice to treat males and females separately in mortality models. Using male mortality data results in lower annuity values and higher market prices of longevity risk since calibrated risk-neutral survival probabilities will be higher and enables us to obtain upper bounds of market prices of longevity risk.

With the assumption that the dynamics of mortality rates are independent of that of interest rates, the BlackRock CORI indexes for the cohorts we will use for determining implied market prices of risk are for cohorts born in $i = 1951, ..., 1960$

$$\begin{aligned} I_x^{CoRI,i}(0) &= \sum_{j=1}^{x^*-65} \bar{P}_x^i(0, 65 - x + j) \\ &= \sum_{j=1}^{x^*-65} P(0, 65 - x + j) S^{Q,i}(x, 0, 65 - x + j), \end{aligned} \tag{23}$$

and for cohorts born in $i = 1941, ..., 1950$

$$\begin{aligned} I_x^{CoRI,i}(0) &= \sum_{j=0}^{x^*-x} \bar{P}_x^i(0, j) \\ &= \sum_{j=0}^{x^*-x} P(0, j) S^{Q,i}(x, 0, j), \end{aligned} \tag{24}$$

where x^* is the maximum age, and is set to 115 by BlackRock.

The market price of longevity risk in the survival function $S^{Q,i}$ (see Equation (9)), can be implied from market prices. Though the longevity market is incomplete, Cairns et al. (2006) suggest that the choice of Λ^i should be consistent with the limited market information. For this reason we calibrate $\lambda_{\mu,1}$, $\lambda_{\mu,2}$, $\lambda_{\mu,3}^i$ ($i = 1941, ..., 1960$) by minimizing differences between our model prices and the BlackRock CORI index values using values at the end of March

2015.

From Equation (9) we see that the risk-neutral survival curve is the best-estimate survival curve multiplied by an adjustment term $e^{C^i(t,T)}$, where $C^i(t,T)$ is a function of the market prices of longevity risk. We continue to group similar cohorts and assume that cohorts born from 1941 to 1950 share the same $\lambda^1_{\mu,3}$ while cohorts born from 1951 to 1960 share the same $\lambda^2_{\mu,3}$. We solve for $\lambda_{\mu,1}$, $\lambda_{\mu,2}$, $\lambda^1_{\mu,3}$ and $\lambda^2_{\mu,3}$ using the following steps:

- calculate yield rate at the end of March 2015 with maturity 1-, 2-, ... 60-year using the AFNS model presented in Equation (11), and then calculate the corresponding discount bond prices;
- simulate best-estimate survival curves for the 20 cohorts born from 1941 to 1960;
- use $\lambda_{\mu,1}$, $\lambda_{\mu,2}$, $\lambda^1_{\mu,3}$ and $\lambda^2_{\mu,3}$ to adjust the best-estimate survival curves and compute index levels for the 20 cohorts;
- find the best $\hat{\lambda}_{\mu,1}$, $\hat{\lambda}_{\mu,2}$, $\hat{\lambda}^1_{\mu,3}$ and $\hat{\lambda}^2_{\mu,3}$ that enable the calculated index level closely match the CoRI index level.

Explicitly we calibrate market price of longevity risk by minimizing the following error term,

$$\hat{\Lambda} = \underset{\Lambda}{\operatorname{argmin}} \sqrt{\sum_{i=1941}^{1960} \left(\hat{I}^i_x(0) - I^{CoRI,i}_x(0) \right)^2}. \tag{25}$$

The calibrated risk premiums are given in Table 6. We see that the first common factor has the highest price of risk. The prices of risk for the second common factor and the two cohort factors are similar with both cohort factors very similar. We note that the CORI indexes imply a higher risk premium for the older cohorts compared to the younger cohorts, which would reflect that the older cohorts are at ages 65 to 74 whose mortality experiences are more volatile.

The resulting risk-neutral model index levels and the values of CoRI indexes published by

BlackRock on 31 March 2015 are shown in Table 7. With the obtained risk premiums, the risk-neutral index level produced by our model closely matches the index level provided by BlackRock. However, there are differences between risk-neutral index level and CoRI index level. The difference decreases across the ten older cohorts and increases across the ten younger cohorts. This suggests an anomaly between our market model and the assumptions underlying the CORI Indexes. This could reflect the higher volatility of mortality of older cohorts, which may lead to a higher longevity risk premium, offset by the decreasing length of payments with the increase in age for the cohorts over an age of 65, which tends to reduce the volatility. The results in Table 7 may reflect that for cohorts born from 1941 to 1950 the second effect dominates while for cohorts born from 1951 to 1960 the first effect dominates.

We analyse the sensitivity of the index level by varying the risk premiums. The cohort survival curve is affected by three market prices of longevity risk. To show this we use scenarios where we vary one market price of longevity risk by 0.01 and fix the other two. ($\hat{\lambda}^1_{\mu,3}$ and $\hat{\lambda}^2_{\mu,3}$ are changed together since they affect different cohorts). The results are presented in Table 8. Higher market prices of longevity risk, corresponding to higher risk-neutral survival probabilities, results in higher risk-neutral index levels, and vice versa. Among the three market prices of longevity risk, $\hat{\lambda}_{\mu,1}$ has the greatest impact on the index level and the impact of varying $\hat{\lambda}_{\mu,2}$ is relatively small. In Figure 6, we also show the differences between the CoRI index level and the risk-neutral index level, at calibrated market prices of longevity risk (given in Table 6) and market prices of longevity risk specified in Scenarios 1 to 6 (given in Table 8). From Figure 6 we observe the same trend that the differences decrease first and increase thereafter, reflecting almost parallel shifts in the index values as the market prices of risk are changed. Varying the first common factor market price of longevity risk causes the greatest change in the differences, which confirms that $\hat{\lambda}_{\mu,1}$ is the most important in determining risk premiums.

Table 6: Calibrated market price of longevity risk.

$\hat{\lambda}_{\mu,1}$	$\hat{\lambda}_{\mu,2}$	$\hat{\lambda}^1_{\mu,3}$	$\hat{\lambda}^2_{\mu,3}$
0.3601	0.0892	0.1099	0.0973

Table 7: CoRI index level and the risk-neutral index level at the market prices of longevity risk given in Table 6.

Cohort	Age	Name	Index level	Risk-neutral index level	Difference
1941	74	CoRI Index 2005	15.26	15.96	0.70
1942	73	CoRI Index 2006	15.94	16.41	0.47
1943	72	CoRI Index 2007	16.61	16.89	0.28
1944	71	CoRI Index 2008	17.28	17.40	0.12
1945	70	CoRI Index 2009	17.95	17.93	-0.02
1946	69	CoRI Index 2010	18.60	18.48	-0.12
1947	68	CoRI Index 2011	19.26	19.05	-0.21
1948	67	CoRI Index 2012	19.93	19.64	-0.29
1949	66	CoRI Index 2013	20.59	20.24	-0.35
1950	65	CoRI Index 2014	21.25	20.85	-0.40
1951	64	CoRI Index 2015	22.19	21.03	-1.16
1952	63	CoRI Index 2016	21.50	20.66	-0.84
1953	62	CoRI Index 2017	20.93	20.29	-0.64
1954	61	CoRI Index 2018	20.35	19.93	-0.42
1955	60	CoRI Index 2019	19.73	19.57	-0.16
1956	59	CoRI Index 2020	19.11	19.21	0.10
1957	58	CoRI Index 2021	18.52	18.85	0.33
1958	57	CoRI Index 2022	17.98	18.50	0.52
1959	56	CoRI Index 2023	17.50	18.13	0.63
1960	55	CoRI Index 2024	16.93	17.77	0.84

*The CoRI Index data is obtained from BlackRock on 31 March 2015.

Table 8: CoRI index level and the risk-neutral index level at various assumptions for the market prices of longevity risk

		Scenarios						
		1	2	3	4	5	6	
$\hat{\lambda}_{\mu,1}$	0.3601	0.3701	0.3501	0.3601	0.3601	0.3601	0.3601	
$\hat{\lambda}_{\mu,2}$	0.0892	0.0892	0.0892	0.0992	0.0792	0.0892	0.0892	
$\hat{\lambda}^1_{\mu,3}$	0.1099	0.1099	0.1099	0.1099	0.1099	0.1199	0.0999	
$\hat{\lambda}^2_{\mu,3}$	0.0973	0.0973	0.0973	0.0973	0.0973	0.1073	0.0873	
Cohort	Risk-neutral index level							CoRI index level
1941	15.96	16.96	15.17	16.13	15.79	16.26	15.67	15.26
1942	16.41	17.36	15.67	16.57	16.25	16.71	16.12	15.94
1943	16.89	17.79	16.18	17.05	16.74	17.20	16.59	16.61
1944	17.40	18.25	16.73	17.55	17.25	17.71	17.10	17.28
1945	17.93	18.74	17.29	18.08	17.79	18.25	17.62	17.95
1946	18.48	19.25	17.87	18.62	18.35	18.81	18.17	18.60
1947	19.05	19.79	18.47	19.19	18.92	19.38	18.73	19.26
1948	19.64	20.34	19.09	19.77	19.51	19.98	19.31	19.93
1949	20.24	20.90	19.71	20.36	20.12	20.58	19.91	20.59
1950	20.85	21.48	20.35	20.97	20.73	21.20	20.51	21.25
1951	21.03	21.59	20.59	21.15	20.93	21.38	20.70	22.19
1952	20.66	21.19	20.24	20.76	20.55	21.00	20.32	21.50
1953	20.29	20.79	19.89	20.39	20.19	20.64	19.95	20.93
1954	19.93	20.40	19.55	20.02	19.83	20.28	19.58	20.35
1955	19.57	20.01	19.21	19.66	19.47	19.92	19.22	19.73
1956	19.21	19.63	18.88	19.30	19.12	19.57	18.86	19.11
1957	18.85	19.25	18.54	18.94	18.77	19.21	18.51	18.52
1958	18.50	18.87	18.20	18.58	18.42	18.85	18.15	17.98
1959	18.13	18.48	17.86	18.21	18.06	18.49	17.79	17.50
1960	17.77	18.10	17.51	17.84	17.70	18.12	17.43	16.93
Total	376.78	389.17	367.01	379.16	374.48	383.54	370.24	377.41

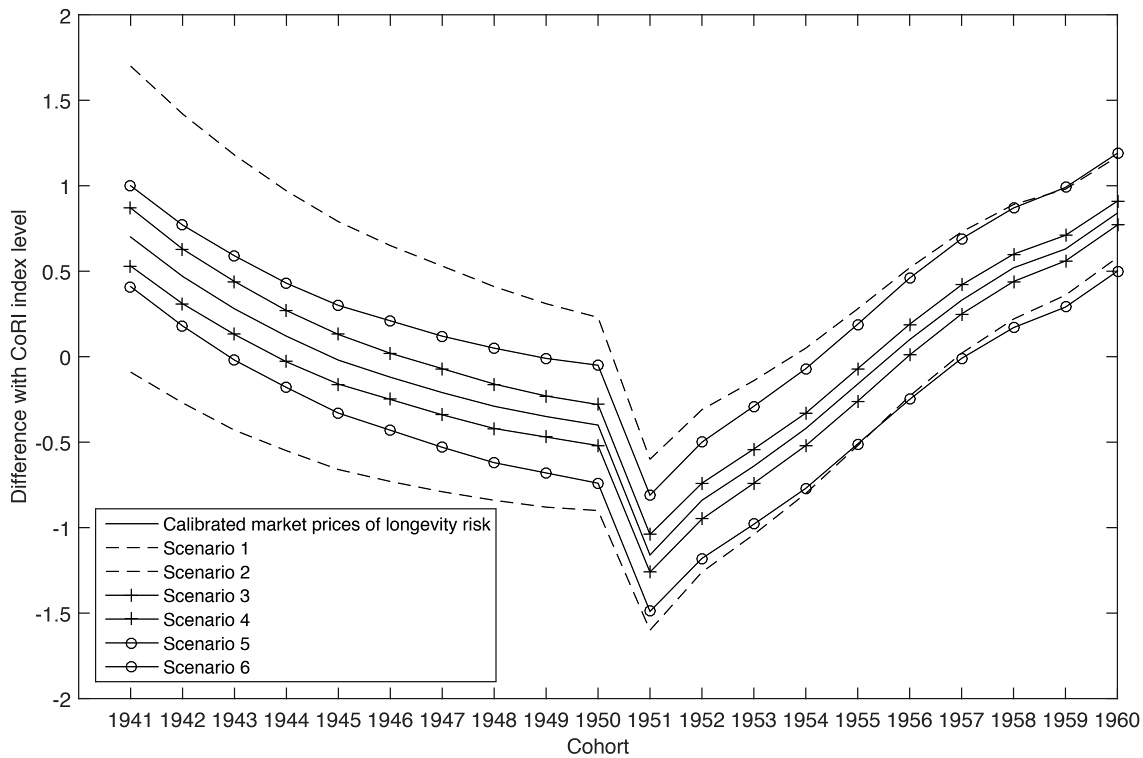

Figure 6: Differences between the CoRI index level and the risk-neutral index level, at calibrated market prices of longevity risk and market prices of longevity risk specified in Scenario 1 to 6.

5 Options on Longevity Bonds

A valuable feature of the continuous time affine mortality model is its tractability in pricing derivatives. In the affine framework, the derivation simplifies considerably and analytical pricing formulas can be obtained. We derive closed–form expressions for prices of European call options written on the longevity zero-coupon bond, $\bar{P}^i_x(t,T)$, as defined in Section 3.3.

5.1 Option Pricing

Consider the value of a call option at time t denoted by $\text{Call}(r,\mu,t,T_C,T)$, where T_C is the exercise date of the option and T is the maturity time of the underlying longevity bond. Note that the underlying asset for the longevity bond option is the longevity zero-coupon bond maturing after the option expires ($T > T_C$). The payoff function for the T_C-maturity call option is

$$\text{Call}(r,\mu,T_C,T_C,T) = \left(\bar{P}^i_x(T_C,T) - K\right)^+, \tag{26}$$

where K is the strike price of the option. The price of the longevity bond option at any time t prior to maturity can be represented as

$$\text{Call}(r,\mu,t,T_C,T) = E^Q\left[\mathrm{e}^{-\int_t^{T_C}\left(r(s)+\mu^i(x,s)\right)ds}\left(\bar{P}^i_x(T_C,T) - K\right)^+ |\mathcal{F}(t)\right], \tag{27}$$

where $E^Q[\cdot]$ denotes the expectation under the risk-neutral measure.

Following Jamshidian (1989) and Geman et al. (1995), we need to remove the stochastic discount factor inside the conditional expectation in Equation (27). This is accomplished by effecting a measure change from the risk-neutral measure to the T_C-forward measure which are linked by the Radon-Nikodym derivative

$$\frac{dQ^{T_C}}{dQ} = \frac{\exp\{-\int_0^{T_C}(r(s)+\mu^i(x,s))ds\}}{\bar{P}^i_x(0,T_C)}. \tag{28}$$

Thus, the price of the longevity bond option at time t becomes

$$\text{Call}(r,\mu,t,T_C,T) = \bar{P}_x^i(t,T_C)E^{T_C}\left[\left(\bar{P}_x^i(T_C,T)-K\right)^+|\mathcal{F}(t)\right], \tag{29}$$

where $E^{T_C}[\cdot]$ denotes the expectation under the T_C-forward measure.

Proposition 1 *The price of a European call option with maturity T and strike K, written on the longevity zero-coupon bond with maturity T_C can be represented as*

$$\begin{aligned} Call(r,\mu,t,T_C,T) &= \bar{P}_x^i(t,T_C)E^{T_C}\left[\left(\bar{P}_x^i(T_C,T)-K\right)^+|\mathcal{F}(t)\right] \\ &= \bar{P}_x^i(t,T_C)\left[e^{M_p+\frac{1}{2}V_p^2}\Phi\left(\frac{M_p-lnK+V_p^2}{V_p}\right)-K\Phi\left(\frac{M_p-lnK}{V_p}\right)\right], \end{aligned} \tag{30}$$

where $\Phi(\cdot)$ is the standard normal cumulative distribution function

$$\begin{aligned} M_p &= V(T_C,T)+A^i(T_C,T)+C^i(T_C,T)-(T-T_C)E^{T_C}\left[L(T_C)|\mathcal{F}(t)\right] \\ &\quad -\left[\frac{1-e^{-\lambda(T-T_C)}}{\lambda}\right]E^{T_C}\left[S(T_C)|\mathcal{F}(t)\right]-\left[\frac{1-e^{-\lambda(T-T_C)}}{\lambda}-e^{-\lambda(T-T_C)}(T-T_C)\right]E^{T_C}\left[C(T_C)|\mathcal{F}(t)\right] \\ &\quad +B_1(T_C,T)E^{T_C}\left[X_1(T_C)|\mathcal{F}(t)\right]+B_2(T_C,T)E^{T_C}\left[X_2(T_C)|\mathcal{F}(t)\right]+B_3^i(T_C,T)E^{T_C}\left[Z^i(T_C)|\mathcal{F}(t)\right], \end{aligned} \tag{31}$$

and

$$\begin{aligned} (V_p)^2 &= s_1^2(T-T_C)^2(T_C-t) \\ &\quad +\left[\frac{1-e^{-\lambda(T-T_C)}}{\lambda}\right]^2\left[\frac{s_2^2}{2\lambda}\left(1-e^{-2\lambda(T_C-t)}\right)+\lambda^2 s_3^2\int_t^{T_C}(T_C-v)^2e^{-2\lambda(T_C-v)}dv\right] \\ &\quad +\frac{s_3^2}{2\lambda}\left[\frac{1-e^{-\lambda(T-T_C)}}{\lambda}-e^{-\lambda(T-T_C)}(T-T_C)\right]^2\left(1-e^{-2\lambda(T_C-t)}\right) \\ &\quad +\frac{\sigma_1^2}{2\phi_1^3}\left(1-e^{-\phi_1(T-T_C)}\right)^2\left(1-e^{-2\phi_1(T_C-t)}\right)+\frac{\sigma_2^2}{2\phi_2^3}\left(1-e^{-\phi_2(T-T_C)}\right)^2\left(1-e^{-2\phi_2(T_C-t)}\right) \\ &\quad +\frac{(\sigma_3^i)^2}{2(\phi_3^i)^3}\left(1-e^{-\phi_3^i(T-T_C)}\right)^2\left(1-e^{-2\phi_3^i(T_C-t)}\right) \end{aligned} \tag{32}$$

with

$$\int_t^{T_C} (T_C - v)^2 e^{-2\lambda(T_C - v)} dv = -\frac{1}{2\lambda}(T_C - t)^2 e^{-2\lambda(T_C - t)} - \frac{1}{2\lambda^2}(T_C - t) e^{-2\lambda(T_C - t)} + \frac{1}{4\lambda^3}\left[1 - e^{-2\lambda(T_C - t)}\right].$$

Proof. See Appendix B. ■

Proposition 2 *The price of a European call option with maturity T and strike K, written on the zero-coupon longevity bond with maturity T_C can be written as*

$$Call(r, \mu, t, T_C, T) = \bar{P}_x^i(t, T)\Phi\left(\frac{ln\frac{\bar{P}_x^i(t,T)}{K\bar{P}_x^i(t,T_C)}}{V_p} + \frac{1}{2}V_p\right) - \bar{P}_x^i(t, T_C)K\Phi\left(\frac{ln\frac{\bar{P}_x^i(t,T)}{K\bar{P}_x^i(t,T_C)}}{V_p} - \frac{1}{2}V_p\right). \quad (33)$$

Proof. Noting that $\frac{\bar{P}_x^i(t,T)}{\bar{P}_x^i(t,T_C)}$ is a martingale under Q^{T_C}, we have

$$\frac{\bar{P}_x^i(t, T)}{\bar{P}_x^i(t, T_C)} = E^{T_C}\left[\bar{P}_x^i(T_C, T)|\mathcal{F}(t)\right] = \mathrm{e}^{M_p + \frac{1}{2}V_p^2}. \quad (34)$$

Substituting Equation (34) into Equation (30) gives the result in the above proposition. ■

Proposition 3 *Following put-call parity,*

$$Call(r, \mu, t, T_C, T) + K\bar{P}_x^i(t, T_C) = Put(r, \mu, t, T_C, T) + \bar{P}_x^i(t, T), \quad (35)$$

the price of a European put option with maturity T and strike K, written on the longevity zero-coupon bond with maturity T_C is given by

$$Put(r, \mu, t, T_C, T) = -\bar{P}_x^i(t, T)\Phi\left(\frac{ln\frac{K\bar{P}_x^i(t,T_C)}{\bar{P}_x^i(t,T)}}{V_p} - \frac{1}{2}V_p\right) + \bar{P}_x^i(t, T_C)K\Phi\left(\frac{ln\frac{K\bar{P}_x^i(t,T_C)}{\bar{P}_x^i(t,T)}}{V_p} + \frac{1}{2}V_p\right). \quad (36)$$

5.2 Options on Zero Coupon Longevity Bonds

Options on zero–coupon longevity bonds differ from those on zero–coupon bonds because of the inclusion of stochastic mortality. Although adding stochastic mortality should increase total volatility and would normally be expected to increase option prices, the effect is more complex than this. Insurers and pension providers who are exposed to longevity risk can reduce their risk by taking long positions in these options.

The closed-form expressions for longevity bond option prices allow us to numerically assess the properties of these derivative prices, which have applications in the hedging of longevity risk. We calculate prices of call options on longevity zero-coupon bonds for the cohort of starting age 55 in 2015, with option maturity being 1-, 2-, 5- and 10-year and bond maturity being 10-, 15-, 20- and 25-year, at parameter values given in Table 1 and 5. We show results of at-the-money (ATM) options together with in-the-money (ITM) and out-of-the-money (OTM) options. When the strike price equals the market price of the underlying longevity zero-coupon bond, the option is at-the-money. The in-the-money strike price is set at 95% of the at-the-money strike price and the out-of-the-money strike price is set at 105% of the at-the-money strike price. Numerical results are given in Table 9. The prices of longevity zero-coupon bond options are compared with the prices of real-rate zero-coupon bond options, the underlying assets of which are real-rate zero-coupon bonds without stochastic mortality.

The impact of stochastic mortality on option prices reflects a number of factors some of which are offsetting and which vary with whether the option is a call option or a put option as well as whether the option is in or out of the money. As noted already stochastic mortality adds to interest rate volatility resulting in higher zero coupon longevity bond call option prices compared to zero coupon bond call option prices. The impact of adding in mortality rates is equivalent to an effective increase in the interest rate for the bond option and higher interest rates mean higher zero coupon longevity bond call option prices with larger increases for in-the-money options and, smaller increases for out-of-the-money options. With the addition of mortality, zero coupon longevity bonds have lower values compared to zero coupon bonds which produces lower strike prices and hence lower call option prices for zero coupon longevity bond call option prices. This effect is larger effect for longer bond maturities.

We see in Table 9 that zero coupon longevity bond call option prices are slightly hump shaped in bond maturity, increasing at first then decreasing, whereas zero coupon bond call option prices are increasing. The difference between the zero coupon bond call options and zero coupon longevity bond call options reduces with option maturity and for a given longevity bond maturity, the bond call option prices increase with increasing option maturity. When option maturity is fixed the price of bond calls increases with bond maturity first and decreases thereafter.

For example, comparing Table 9 with Table 10, we note that for shorter bond maturities, such as 10 and 15 years, real-rate zero-coupon bond options are cheaper than longevity zero-coupon bond options since bond option prices are decreasing functions of the volatility of underlying processes. However, for longer maturities, for example 25 years, longevity zero-coupon bond options become cheaper. The decreasing survival probability reduces the strike price of longevity zero-coupon bond options, which tends to reduce the call option price. The price of a 25-year real-rate zero-coupon bond is 0.8678 while the price of a longevity zero-coupon bond is only 0.5582 with the same maturity.

6 Conclusion

In this paper, we have applied a continuous time affine multi–cohort mortality model along with an AFNS interest rate model to imply market prices of longevity risk from the Black-Rock CoRI Retirement Indexes. Our models are affine and allow closed-form expressions for survival probabilities and zero-coupon bond prices. Market prices of longevity risk can be readily incorporated in this model framework since we have formula for arbitrage–free prices

Table 9: Prices of a set of call options on longevity zero-coupon bonds for the cohort of starting age 55 in 2015, at the market price of longevity risk given in Table 6.

		Option maturity			
Bond maturity	Zero-coupon longevity bond	1	2	5	10
ATM					
10	0.9203	0.0303	0.0394	0.0488	-
15	0.8397	0.0396	0.0530	0.0717	0.0830
20	0.7197	0.0435	0.0589	0.0829	0.0993
25	0.5582	0.0407	0.0556	0.0800	0.0986
ITM					
10	-	0.0593	0.0675	0.0797	-
15	-	0.0639	0.0763	0.0954	0.1132
20	-	0.0632	0.0778	0.1015	0.1201
25	-	0.0555	0.0697	0.0935	0.1129
OTM					
10	-	0.0127	0.0204	0.0267	-
15	-	0.0226	0.0352	0.0524	0.0578
20	-	0.0285	0.0436	0.0670	0.0811
25	-	0.0291	0.0438	0.0681	0.0859

Table 10: Prices of a set of call options on real-rate zero-coupon bonds in 2015, without mortality component.

		Option maturity			
Bond maturity	Zero-coupon bond	1	2	5	10
ATM					
10	0.9859	0.0208	0.0255	0.0258	-
15	0.9596	0.0319	0.0412	0.0511	0.0437
20	0.9210	0.0417	0.0553	0.0739	0.0767
25	0.8678	0.0498	0.0670	0.0930	0.1050
ITM					
10	-	0.0531	0.0556	0.0563	-
15	-	0.0604	0.0680	0.0771	0.0740
20	-	0.0675	0.0796	0.0972	0.1014
25	-	0.0731	0.0890	0.1139	0.1263
OTM					
10	-	0.0054	0.0090	0.0090	-
15	-	0.0143	0.0229	0.0320	0.0229
20	-	0.0238	0.0369	0.0551	0.0567
25	-	0.0324	0.0494	0.0753	0.0867

of longevity-linked products.

The models allow us to imply market prices of risk from the BlackRock CORI indexes for both common factors and cohort based factors in our mortality model. We show that there are differences between our risk-neutral model index values and the CORI indexes. For both younger and older cohorts the CORI Indexes are lower than our values and higher for cohorts around age 65. We explain this by potential differences in the treatment of mortality risk in the computation of the CORI indexes.

Closed-form pricing formulas are derived for longevity zero-coupon bond options. We show that the impact of stochastic mortality on option prices on longevity bonds is complex and requires the consideration of effects from stochastic mortality arising from volatility, effective interest rates, and strike prices. We show this by comparing the prices of longevity zero-coupon bond options with the prices of real-rate zero-coupon bond options. For shorter bond maturities real-rate zero-coupon bond options are cheaper while for longer maturities longevity zero-coupon bond options become cheaper.

Appendix

A. Kalman Filter Algorithm

The measurement equation is

$$y_t = -BY_t - A + \varepsilon_t, \qquad \varepsilon_t \sim N(0, H), \tag{37}$$

where A and B are given by (18) and (21), H is a diagonal matrix with elements $\sigma_\varepsilon^2(\tau_i)$. The state transition equation can be represented as

$$Y_t = a + bY_{t-1} + \eta_t, \qquad \eta_t \sim N(0, Q), \tag{38}$$

where a, b and Q are given by (20) and (22).

Denote the filtered values of the state variables and their corresponding covariance matrix by $Y_{t|t}$ and $S_{t|t}$, and further denote the unknown parameters by θ. In the forecasting step, we forecast unknown values of state variables conditioning on the information at time $t-1$ such that

$$Y_{t|t-1} = a + bY_{t-1|t-1}, \tag{39}$$

$$S_{t|t-1} = b' S_{t-1|t-1} b + Q_t(\theta). \tag{40}$$

In the next step we use the information at time t to update our forecasts

$$Y_{t|t} = Y_{t|t-1} - S_{t|t-1} B(\theta) F_{t|t-1}^{-1} v_{t|t-1}, \tag{41}$$

$$S_{t|t} = S_{t|t-1} - S_{t|t-1} B(\theta) F_{t|t-1}^{-1} B(\theta)' S_{t|t-1}, \tag{42}$$

where

$$v_{t|t-1} = y_t + A(\theta) + B(\theta)X_{t|t-1},$$
$$F_{t|t-1} = B(\theta)' S_{t|t-1} B(\theta) + H.$$

Every iteration will yield a value for the log-likelihood function shown below

$$\log l(y_1, ..., y_T; \theta) = \sum_{t=1}^{T} \left(-\frac{N}{2} \log(2\pi) - \frac{1}{2} \log(F_{t|t-1}) - \frac{1}{2} v'_{t|t-1} F^{-1}_{t|t-1} v_{t|t-1} \right), \tag{43}$$

where N is the number of observed time series. The estimated parameter set $\hat{\theta}$ is determined as the one which maximizes the log-likelihood function.

B. Proof of Proposition 1

The following derivations are based on Theorem 4.2.2 in Brigo and Mercurio (2013). From Equation (14) we know that

$$\begin{aligned}
\bar{P}^i_x(T_C, T) &= P(t,T) S^{Q,i}(x,t,T) \\
&= \exp\Big\{ V(T_C,T) - (T - T_C)L(T_C) - \frac{1 - e^{-\lambda(T-T_C)}}{\lambda} S(T_C) \\
&\quad - \left[\frac{1 - e^{-\lambda(T-T_C)}}{\lambda} - e^{-\lambda(T-T_C)}(T - T_C) \right] C(T_C) \\
&\quad + A^i(T_C,T) + C^i(T_C,T) + B_1(T_C,T)X_1(T_C) + B_2(T_C,T)X_2(T_C) + B^i_3(T_C,T)Z^i(T_C) \Big\},
\end{aligned} \tag{44}$$

where $L(T_C)$, $S(T_C)$ and $C(T_C)$ are the values of level, slope and curvature factors of the interest rate dynamics at time T_C, and $X_1(T_C)$, $X_2(T_C)$ and $Z^i(T_C)$ are the values of mortality factors at time T_C.

As a result, under the T_C-forward measure the logarithm of $\bar{P}^i_x(T_C, T)$ conditional on $\mathcal{F}(t)$

is normally distributed with mean

$$M_p = V(T_C,T) + A^i(T_C,T) + C^i(T_C,T) - (T-T_C)E^{T_C}\left[L(T_C)|\mathcal{F}(t)\right] - \left[\frac{1-e^{-\lambda(T-T_C)}}{\lambda}\right]E^{T_C}\left[S(T_C)|\mathcal{F}(t)\right] - \left[\frac{1-e^{-\lambda(T-T_C)}}{\lambda} - e^{-\lambda(T-T_C)}(T-T_C)\right]E^{T_C}\left[C(T_C)|\mathcal{F}(t)\right] + B_1(T_C,T)E^{T_C}\left[X_1(T_C)|\mathcal{F}(t)\right] + B_2(T_C,T)E^{T_C}\left[X_2(T_C)|\mathcal{F}(t)\right] + B_3^i(T_C,T)E^{T_C}\left[Z^i(T_C)|\mathcal{F}(t)\right] \tag{45}$$

and variance

$$\begin{aligned}(V_p)^2 &= s_1^2(T-T_C)^2(T_C-t) \\ &+ \left[\frac{1-e^{-\lambda(T-T_C)}}{\lambda}\right]^2\left[\frac{s_2^2}{2\lambda}\left(1-e^{-2\lambda(T_C-t)}\right) + \lambda^2 s_3^2\int_t^{T_C}(T_C-v)^2\mathrm{e}^{-2\lambda(T_C-v)}dv\right] \\ &+ \frac{s_3^2}{2\lambda}\left[\frac{1-e^{-\lambda(T-T_C)}}{\lambda} - e^{-\lambda(T-T_C)}(T-T_C)\right]^2\left(1-e^{-2\lambda(T_C-t)}\right) \\ &+ \frac{\sigma_1^2}{2\phi_1^3}\left(1-e^{-\phi_1(T-T_C)}\right)^2\left(1-e^{-2\phi_1(T_C-t)}\right) + \frac{\sigma_2^2}{2\phi_2^3}\left(1-e^{-\phi_2(T-T_C)}\right)^2\left(1-e^{-2\phi_2(T_C-t)}\right) \\ &+ \frac{(\sigma_3^i)^2}{2(\phi_3^i)^3}\left(1-e^{-\phi_3^i(T-T_C)}\right)^2\left(1-e^{-2\phi_3^i(T_C-t)}\right),\end{aligned} \tag{46}$$

where

$$\begin{aligned}\int_t^{T_C}(T_C-v)^2\mathrm{e}^{-2\lambda(T_C-v)}dv &= -\frac{1}{2\lambda}(T_C-t)^2\mathrm{e}^{-2\lambda(T_C-t)} - \frac{1}{2\lambda^2}(T_C-t)\mathrm{e}^{-2\lambda(T_C-t)} \\ &\quad + \frac{1}{4\lambda^3}\left[1-\mathrm{e}^{-2\lambda(T_C-t)}\right].\end{aligned} \tag{47}$$

Since

$$\begin{aligned}&\int_{-\infty}^{+\infty}\frac{1}{\sqrt{2\pi}V_p}\left(\mathrm{e}^z-K\right)^+\mathrm{e}^{-\frac{(z-M_p)^2}{V_p^2}}dz \\ &\quad = \mathrm{e}^{M_p+\frac{1}{2}V_p^2}\Phi\left(\frac{M_p-\ln K+V_p^2}{V_p}\right) - K\Phi\left(\frac{M_p-\ln K}{V_p}\right),\end{aligned} \tag{48}$$

we have that

$$
\begin{aligned}
\mathrm{Call}(r,\mu,t,T_C,T) &= \bar{P}_x^i(t,T_C)E^{T_C}\left[\left(\bar{P}_x^i(T_C,T)-K\right)^+|\mathcal{F}(t)\right] \\
&= \bar{P}_x^i(t,T_C)\left[\mathrm{e}^{M_p+\frac{1}{2}V_p^2}\Phi\left(\frac{M_p-\ln K+V_p^2}{V_p}\right)-K\Phi\left(\frac{M_p-\ln K}{V_p}\right)\right], \quad (49)
\end{aligned}
$$

where $\Phi(\cdot)$ is the standard normal cumulative distribution function.

References

Bauer, D., Börger, M., and Ruß, J. (2010). On the pricing of longevity-linked securities. *Insurance: Mathematics and Economics*, 46(1):139–149.

Bauer, D. and Ruß, J. (2006). Pricing longevity bonds using implied survival probabilities. In *2006 meeting of the American Risk and Insurance Association (ARIA)*.

Blackburn, C. and Sherris, M. (2013). Consistent dynamic affine mortality models for longevity risk applications. *Insurance: Mathematics and Economics*, 53:64–73.

Blake, D. and Burrows, W. (2001). Survivor bonds: Helping to hedge mortality risk. *Journal of Risk and Insurance*, 68(2):339–348.

Brigo, D. and Mercurio, F. (2013). *Interest Rate Models Theory and Practice*. Springer Science & Business Media.

Cairns, A. J., Blake, D., and Dowd, K. (2006). A two-factor model for stochastic mortality with parameter uncertainty: Theory and calibration. *Journal of Risk and Insurance*, 73(4):687–718.

Chigodaev, A., Milevsky, M. A., and Salisbury, T. S. (2016). How long does the market think you will live? implying longevity from annuity prices. *The Journal of Investment Consulting*, 17(1):11–21.

Christensen, J. H., Diebold, F. X., and Rudebusch, G. D. (2011). The affine arbitrage-free class of nelson–siegel term structure models. *Journal of Econometrics*, 164(1):4–20.

Coughlan, G., Epstein, D., Sinha, A., and Honig, P. (2007). q-forwards: Derivatives for transferring longevity and mortality risks. *JPMorgan Pension Advisory Group, London, July*, 2.

Dai, Q. and Singleton, K. J. (2000). Specification analysis of affine term structure models. *The Journal of Finance*, 55(5):1943–1978.

Diebold, F. X. and Li, C. (2006). Forecasting the term structure of government bond yields. *Journal of Econometrics*, 130(2):337–364.

Dowd, K., Blake, D., Cairns, A. J., and Dawson, P. (2006). Survivor swaps. *Journal of Risk and Insurance*, 73(1):1–17.

Duffee, G. R. (2002). Term premia and interest rate forecasts in affine models. *The Journal of Finance*, 57(1):405–443.

Duffie, D., Kan, R., et al. (1996). A yield-factor model of interest rates. *Mathematical Finance*, 6:379–406.

Geman, H., El Karoui, N., and Rochet, J.-C. (1995). Changes of numeraire, changes of probability measure and option pricing. *Journal of Applied Probability*, pages 443–458.

Jamshidian, F. (1989). An exact bond option formula. *The Journal of Finance*, 44(1):205–209.

Jevtic, P., Luciano, E., and Vigna, E. (2013). Mortality surface by means of continuous time cohort models. *Insurance: Mathematics and Economics*, 53:122–133.

Lin, Y. and Cox, S. H. (2005). Securitization of mortality risks in life annuities. *Journal of Risk and Insurance*, 72(2):227–252.

Nelson, C. R. and Siegel, A. F. (1987). Parsimonious modeling of yield curves. *Journal of Business*, pages 473–489.

Schönbucher, P. J. (2003). *Credit derivatives pricing models: models, pricing and implementation.* John Wiley & Sons.

Xu, Y., Sherris, M., and Ziveyi, J. (2015). The application of affine processes in multi-cohort mortality models. Working paper, UNSW Business School Research Paper.